Long-lived fermionic Feshbach molecules with tunable *p*-wave interactions

Marcel Duda [1,2,*], Xing-Yan Chen [1,2,*], Roman Bause [1,2], Andreas Schindewolf [1,2]
Immanuel Bloch [1,2,3] and Xin-Yu Luo [1,2,†]

[1]*Max-Planck-Institut für Quantenoptik, 85748 Garching, Germany*
[2]*Munich Center for Quantum Science and Technology, 80799 München, Germany*
[3]*Fakultät für Physik, Ludwig-Maximilians-Universität, 80799 München, Germany*

Ultracold fermionic Feshbach molecules are promising candidates for exploring quantum matter with strong *p*-wave interactions; however, their lifetimes were measured to be short. Here we characterize the *p*-wave collisions of ultracold fermionic ^{23}Na ^{40}K Feshbach molecules for different scattering lengths and temperatures. By increasing the binding energy of the molecules, the two-body loss coefficient reduces by three orders of magnitude, leading to a second-long lifetime 20 times longer than that of ground-state NaK molecules. We exploit the scaling of elastic and inelastic collisions with the scattering length and temperature to identify a regime where the elastic collisions dominate over the inelastic ones, allowing the molecular sample to thermalize. Our results provide a benchmark for four-body calculations of molecular collisions and pave the way for investigating quantum many-body phenomena with fermionic Feshbach molecules.

I. INTRODUCTION

Ultracold molecules have gained considerable attention in the past years. Their rich internal structure offers unique opportunities for quantum-engineering and quantum-chemistry applications [1–3]. However, a major challenge for their usability to investigate quantum many-body physics is to identify interacting molecular systems where the undesired collisional loss processes are under control.

A promising platform are optically trapped Feshbach molecules which are formed through an atomic interspecies Feshbach resonance [4]. These molecules do not only represent a key intermediate product for generating ground-state polar molecules, but also are intriguing due to their rich collisional behavior near the Feshbach resonance. When the molecules are weakly bound and the wave function extends beyond the interatomic potential, the only relevant length scale in the system is the interspecies scattering length. It determines the size of the dimers and the interactions between them in the so-called universal halo regime [5]. Molecules composed of one boson and one fermion are especially interesting as the dominating collision channel in these composite fermions is *p* wave. As a consequence, the molecules are protected by a centrifugal *p*-wave barrier from reaching short range and undergoing inelastic loss. In addition, a theoretical

study has shown that the elastic *p*-wave collisions drastically increase with the interspecies scattering length and with temperature. These scalings are expected to be stronger than those for the inelastic collisions [6]. In contrast, the ratio of elastic-to-inelastic collisions in spin-polarized fermionic atoms reduces with increasing *p*-wave interactions due to enhanced three-body losses [7]. Therefore, fermionic Feshbach molecules are promising to realize unconventional superfluidity [8,9].

However, common wisdom dictates that Feshbach molecules, being in a highly excited vibrational state, should be short lived, especially when compared to molecules in the rovibronic ground state. In addition, unlike bosonic molecules composed of fermions [10,11], Pauli blocking does not protect fermionic Feshbach molecules from undergoing three-body loss, involving two bosons and one fermion colliding at short range. The collisional instability of fermionic Feshbach molecules was confirmed in experiments where lifetimes on the order of hundred milliseconds [12,13] or as short as a millisecond [14] were measured. Due to the short lifetime of these molecules, so far no experimental evidence for elastic *p*-wave collisions could be provided, despite the predicted favorable scaling of elastic-to-inelastic collisions with temperature and scattering length. In addition, calculating four-body collisions is highly nontrivial. Only in the extreme case that one constituent atom is much lighter than the other can the collisions be reduced to a three-body problem under the Oppenheimer approximation. However, these calculations are only considered to be valid in the halo regime [6]. It is not clear whether the predictions apply to molecules consisting of two atoms with comparable mass and how the collision properties change away from the halo regime.

In this work we realize tunable *p*-wave interactions in a trapped sample of fermionic NaK Feshbach molecules. By tuning the magnetic field close to an atomic *s*-wave Feshbach

resonance, the Feshbach molecules enter the halo regime, where they feature strong *p*-wave interactions. We observe that the inelastic collision rates can be changed by three orders of magnitude, and we see indication of an even higher tunability for the elastic collision rates. While the inelastic collision rates follow closely the expected universal *p*-wave scaling to scattering length and temperature in the deep halo or nonhalo regime, nonuniversal behavior occurs in the intermediate regime, indicating a potential Efimov resonance [15].

II. INELASTIC COLLISIONS

In a first set of measurements, we characterize the loss between NaK Feshbach molecules which occurs when the molecules overcome the centrifugal *p*-wave barrier. Once they reach the short-range regime, the loss can be described by Na-Na-K three-body recombination, where the additional K atom acts as a spectator and carries away the kinetic energy on the order of the Feshbach-molecule binding energy [16]. The inelastic collision rate is determined by the barrier height V_b and the collision energy E_c and is proportional to $(E_c/V_b)^{3/2}$ [17]. In the halo regime and in absence of an Efimov resonance, Marcelis *et al.* calculated that $V_b \propto a^{-2}$ and, therefore, the loss rate scales with $a^3 T$ [6]. Here a is the *s*-wave interspecies scattering length and T is the temperature of the sample. In comparison, the elastic collision cross section is proportional to $V_p^2 T^2$, where V_p is the *p*-wave scattering volume. Under the same approximation, Marcelis *et al.* calculated that $V_p \propto a^3$. Therefore elastic collision rates are predicted to scale with $a^6 T^{2.5}$. However, as we will show later, the *p*-wave scattering volume might not be strictly defined for all measured scattering lengths, for example, when the collisional behavior deviates from the universal *p*-wave collisions due to Efimov resonances. To make the least assumptions about the system, we characterize the collisions in terms of collision rates as a function of the interspecies scattering length.

We start from a mixture of bosonic ^{23}Na and fermionic ^{40}K atoms in their respective energetically lowest hyperfine states $|F, m_F\rangle = |1, 1\rangle$ and $|9/2, -9/2\rangle$, where F represents the total angular momentum and m_F the projection onto the magnetic-field axis. To associate Feshbach molecules, we ramp the magnetic field across an interspecies Feshbach resonance at 78.3 G, which we have previously characterized [18], followed by an additional fast magnetic-field ramp to 72.3 G where the Feshbach molecules have a vanishing magnetic moment. As the remaining atoms possess a finite magnetic moment, we remove them from the trap by applying a magnetic-field gradient of 40 G/cm. This procedure typically produces 3×10^4 Feshbach molecules at a temperature of 500 nK in a crossed optical dipole trap. The trapping frequencies are $(\omega_x, \omega_y, \omega_z) = 2\pi \times (57, 91, 246)$ Hz, where the *z* direction is the direction along gravity.

We investigate the dependence of the collisional loss on the scattering length by ramping the magnetic field to the target magnetic field B, where we hold the molecules for a variable time. For detection we first turn off all dipole traps, then ramp the magnetic field back through the Feshbach resonance to dissociate the molecules. Finally, the dissociated atoms are detected in time of flight using absorption imaging. The imaging beam propagates along the *y* direction, allowing us to extract the temperatures in the *x* and *z* direction.

We fit the loss of Feshbach molecules in a harmonic trap with the two-body loss model,

$$\frac{dN}{dt} = -\frac{\beta_{\text{inel}} N^2}{v_0 T^{3/2}}, \tag{1}$$

where β_{inel} is the inelastic collision coefficient, N is the number of molecules, $v_0 T^{3/2}$ is the generalized trap volume given by $v_0 = (4\pi k_B/m\bar{\omega}^2)^{3/2}$, with $\bar{\omega} = (\omega_x \omega_y \omega_z)^{1/3}$ the geometric mean of the trap frequencies, k_B the Boltzmann constant, and m the mass of molecules. Since we do not observe a significant change of the temperature during the measurement, we do not include any heating effects in our model. We also ignore the inelastic collisions between Feshbach molecules and spectator K atoms that remain in the trap close to the resonance where their collisions are strongly suppressed by Pauli blocking [12,19].

We extract the interspecies scattering length from the magnetic field using a model with two overlapping Feshbach resonances given by

$$a(B) = a_{bg} \left(\frac{B - B_1^*}{B - B_{0,1}} \right) \left(\frac{B - B_2^*}{B - B_{0,2}} \right), \tag{2}$$

where $a_{bg} = -619 a_0$ [20] is the background scattering length, $B_{0,1} = 78.3$ G and $B_{0,2} = 89.7$ G are the two resonance positions, and $B_1^* = 73.03$ G and $B_2^* = 80.36$ G are the zero crossings of the scattering length [18].

Our findings of β_{inel} as a function of a are summarized in Fig. 1. In the halo regime, we observe a strong dependence of the loss coefficient β_{inel} on the scattering length. We check the scaling by fitting the two-body loss coefficient with a polynomial of the form $\beta_{\text{inel}}(a) = ca^{l_a}$ for scattering lengths $a > 1000 a_0$ and obtain $l_a = 2.58(14)$. We note that not all data points used for the fit are deep enough in the halo regime to exhibit the predicted a^3 scaling. In fact, as shown in Appendix A, the locally extracted *a*-scaling exponent l_a still increases for $a > 1500 a_0$ [19]. All measured rates of inelastic collisions are below the unitarity limit $\beta_{\text{unitary}} = 2\hbar\lambda_{dB}/\mu$ [22], which corresponds to a value of $\beta = 1.77 \times 10^{-9}$ cm^3/s at a temperature of 500 nK. Here λ_{dB} corresponds to the the de Broglie wavelength of a molecule and μ to the reduced mass of the molecule pair. Interestingly, the loss coefficient does not seem to saturate to the unitarity limit close to resonance. We believe that two reasons might contribute to this: First, the changes in l_a might mask the onset of the saturation. Second, in this regime β_{inel} might be overestimated by up to 15% because of additional loss that stems from an accumulation of Na atoms, as discussed in Appendix B.

For $a < 1000 a_0$, the effect of the scattering length on the loss rate is weaker. In particular, once the molecules are deep in the nonhalo regime where a is smaller than the van der Waals length a_{vdW}, the two-body loss approaches $\beta_{\text{inel}} = (3.3 \pm 0.1^{\text{stat.}} \pm 1.1^{\text{sys.}}) \times 10^{-12}$ cm^3/s [see Fig. 1(b)]. We compare this value to the predictions from multichannel quantum defect theory (MQDT), which have previously reproduced the loss coefficient for molecules in rovibronic ground states [21,23] and in high-lying vibrational states [24]. The predicted two-body loss coefficient in collisions of indis-
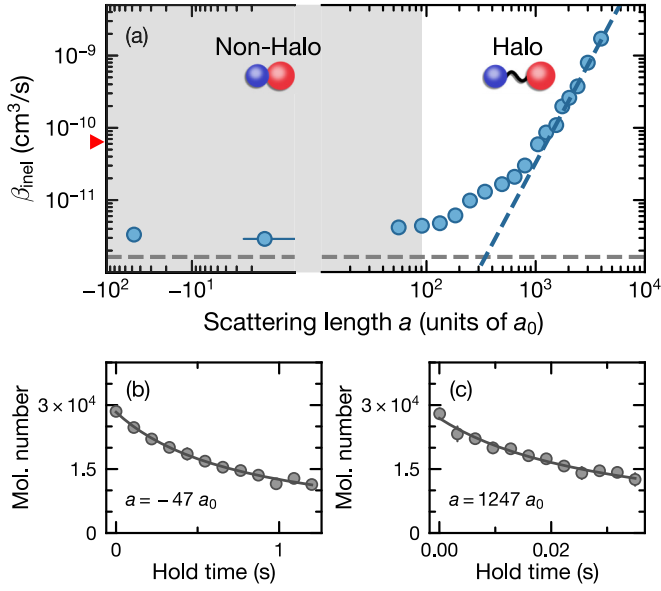
FIG. 1. Two-body loss coefficient β_{inel} as a function of the scattering length a for $T = 500$ nK. (a) Deep in the nonhalo regime the loss approaches $\beta_{inel} = (3.3 \pm 0.1^{stat.} \pm 1.1^{sys.}) \times 10^{-12}$ cm^3/s. The gray dashed line indicates the loss coefficient of $\beta_{inel} = 1.65 \times 10^{-12}$ cm^3/s predicted by MQDT calculations. For $a > 1000\, a_0$, β_{inel} is fitted with $\beta_{inel}(a) = ca^{l_a}$, which yields $l_a = 2.58(14)$ (blue dashed line). The red triangle indicates the coefficient of inelastic collisions in NaK ground-state molecules for $T = 500$ nK [21]. The statistical error in β_{inel} is given by the error of the fit. A systematic error of 30% in β_{inel} is expected from a 10% error in the trapping frequency. The horizontal error bars result from a 15-mG uncertainty in the magnetic field. (b, c) The number of Feshbach molecules as a function of the hold time for $B = 72$ G ($a = -47\, a_0$) and $B = 77.8$ G ($a = 1300\, a_0$). The solid line shows the fitted molecule number from the two-body loss model described by Eq. (1), assuming a constant temperature.

tinguishable fermions is given by

$$\beta_{inel}(T) = \frac{\Gamma(1/4)^6}{\Gamma(3/4)^2} \bar{a}^3 \frac{k_B T}{h} = 1513 \bar{a}^3 \frac{k_B T}{h}, \qquad (3)$$

where $\bar{a} = 2\pi(2\mu C_6/\hbar^2)^{1/4}/\Gamma(\frac{1}{4})^2 = 88.8\, a_0$ is the average scattering length, C_6 is the van der Waals coefficient, and $\Gamma(x)$ is the gamma function [25]. The average scattering length $\bar{a} = 0.956\, a_{vdW}$ can be understood as the size of the molecule in the nonhalo regime. We calculate the van der Waals coefficient of NaK Feshbach molecules by approximating the long-range interaction to be the sum of the contribution from individual atoms, i.e., $C_{6,FB} = C_{6,Na} + C_{6,K} + 2C_{6,Na-K}$, where $C_{6,Na} = 1556$, $C_{6,K} = 3897$ [26], and $C_{6,Na-K} = 2454$ [27] in atomic units. At a temperature of 500 nK, Eq. (3) then yields 1.65×10^{-12} cm^3/s, which is a factor of 2 lower than the measured value. The deviation from the universal limit can be attributed either to the 30% systematic uncertainty of the measurements or to nonunity loss probability at the short range. In the latter case, reflection from the short range can interfere with the incoming molecular wave function, thereby enhancing or reducing the loss rate [25].

We note that the two-body loss coefficient of NaK Feshbach molecules in the nonhalo regime is 20 times lower than that of the ground-state molecules [21]. This contra-
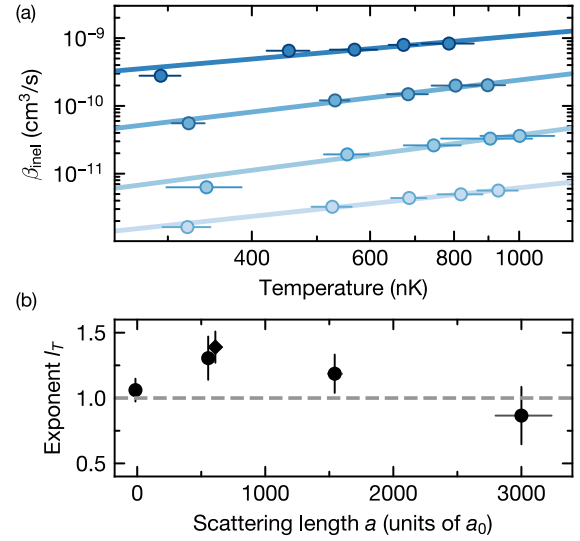

FIG. 2. Temperature-dependent collisional loss of Feshbach molecules. (a) The coefficient β_{inel} is shown for various temperatures at $a = -14\, a_0$, $554\, a_0$, $1542\, a_0$, $3000\, a_0$ (from bright to dark blue). The loss coefficient obtained from the respective data sets are fitted with a polynomial of the form cT^{l_T} (solid lines). The statistical error in β_{inel} is given by the error of the fit. A systematic error of 30% in β_{inel} is expected from a 10% error in the trapping frequency. The horizontal error bars represent the statistical error of of T_{avg} during the hold time. (b) Extracted exponent l_T as function of the scattering length. The vertical error bars represent error of the fit, and the horizontal error bars are the error in the scattering length. The gray dashed line is a guide to the eye corresponding to a linear temperature scaling. The distinct data point (diamond) corresponds to the temperature scaling of the loss in Fig. 4.

dicts the naive expectation that the rovibronic ground-state molecules should live longer than the weakly bound Feshbach molecules. However, this can be explained by considering that the strong molecule-frame dipole moment d present in ground-state molecules modifies the van der Waals interaction. This effectively increases the van der Waals length for ground-state molecules and thus the universal two-body loss coefficient [28]. The agreement of the loss coefficients for ground-state and Feshbach molecules with these models strongly suggests that the lifetime of fermionic NaK molecules is determined by the long-range interaction potential, regardless of the loss mechanism at short range.

Next we study the temperature dependence of the collisional loss. We achieve different temperatures between 300 nK and 1000 nK by adiabatically compressing or decompressing the trap before the loss measurement. As shown in Fig. 2, β_{inel} increases with temperature for all data sets. We fit a polynomial of the form cT^{l_T} to the loss coefficient. The data is closely approximated by a linear fit [see Fig. 2(b)]. However, especially in the regime close to $500\, a_0$, the scaling seems to be stronger than linear. Anomalous temperature dependence of inelastic collisions was also observed in bosonic Feshbach molecules such as Cs$_2$ and NaRb at around $500\, a_0$, and its origin is still unclear [5,29]. In addition to the anomalous temperature dependence of β_{inel}, an enhanced loss of β_{inel} as a function of the scattering length occurs at around $500\, a_0$,

as shown in Fig. 1. We speculate that the deviations result from a Na-Na-K Efimov resonance, which also shows up in the rate coefficient of atom-dimer collisions in Appendix B.

III. ELASTIC COLLISIONS

In the second set of measurements, we investigate elastic collisions between Feshbach molecules. As introduced in the previous section, the elastic collision rate is predicted to scale as $a^6 T^{2.5}$ in the halo regime if Efimov resonances are absent [6]. Thus we expect that elastic collisions dominate over inelastic collisions for high temperatures and large scattering lengths, such that a molecular sample out of equilibrium can rethermalize during its lifetime. We create such an out-of-equilibrium molecular sample by nonadiabatically compressing the optical dipole trap after the molecule association such that the trapping frequencies ω_y, ω_z increase more than ω_x. After compressing the trap at 77 G, we ramp the magnetic field to the target magnetic field B within 1.5 ms. where we hold the molecules for a variable time. We typically produce 1×10^4 Feshbach molecules with an initial temperature of $T_x = 350$ nK and $T_z = T_y = 550$ nK.

To obtain both the elastic and inelastic collision coefficients, we adapt the model used for two-body collisions in polar molecules [30] to obtain the following set of differential equations:

$$\frac{dn}{dt} = -\frac{n^2}{3}K_{\text{inel}}(2T_z + T_x) - \frac{n}{2T_x}\frac{dT_x}{dt} - \frac{n}{2T_z}\frac{dT_z}{dt}, \quad (4)$$

$$\frac{dT_z}{dt} = \frac{n}{12}K_{\text{inel}}T_zT_x - \frac{\Gamma_{th}}{3}(T_z - T_x) + c_l, \quad (5)$$

$$\frac{dT_x}{dt} = \frac{n}{12}K_{\text{inel}}(2T_z - T_x)T_x + \frac{2\Gamma_{th}}{3}(T_z - T_x) + c_l. \quad (6)$$

Here n is the average density of the sample, and $K_{\text{inel}} = \beta_{\text{inel}}/T$ is the temperature-independent coefficient of inelastic collisions. T_x and T_z are the effective temperatures of the molecules in the horizontal and vertical direction, respectively. We checked that the temperature along the direction of the imaging beam T_y is equal to T_z and assume this for all measurements. Γ_{th} is the thermalization rate given by $\Gamma_{th} = n\sigma\bar{v}/\alpha$, where σ is the cross section of the elastic collisions, which is assumed to be constant for each measurement, $\bar{v} = \sqrt{16k_B(2T_z + T_x)/(3\pi m)}$ is the average velocity of molecules, and $\alpha = 4.1$ is the number of collisions needed for thermalization in p-wave collisions [30,31]. The linear heating term c_l has been introduced to phenomenologically account for isotropic heating that we observe in these measurements. We numerically fit Eqs. (4)–(6) in the basis of the average temperature $T_{\text{avg}} = (2T_z + T_x)/3$ and the difference in temperature $\Delta T = T_z - T_x$ to reduce the common mode fluctuation in the temperatures.

The resulting coefficients of inelastic and elastic collisions, β_{inel} and $\beta_{\text{el}} = \sigma\bar{v}$, are summarized in Fig. 3 as a function of the scattering length for a temperature of 500 nK. Deep in the nonhalo regime, collisions of Feshbach molecules predominantly result in loss such that the number of elastic collisions during the lifetime of the molecular sample is negligible. As a result, cross-dimensional thermalization is absent [see Fig. 3(b)]. For higher scattering lengths the elastic collision rate increases notably faster than the inelastic collision rate.
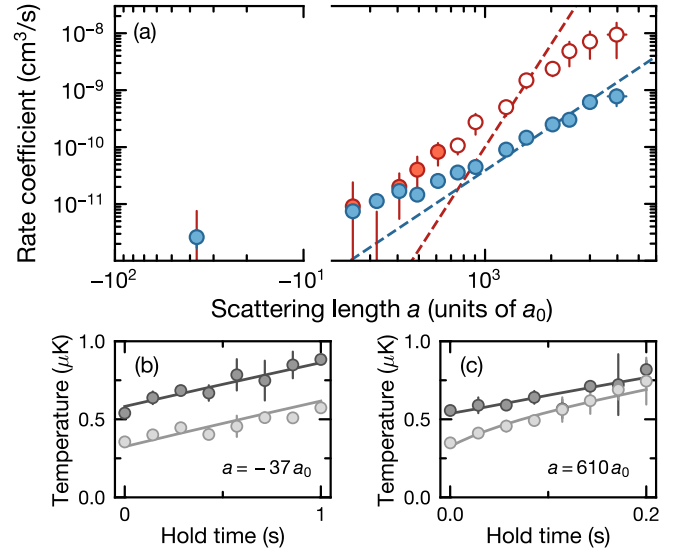

FIG. 3. Elastic p-wave collisions of fermionic Feshbach molecules. (a) Elastic collision coefficient β_{el} (red) and inelastic collision coefficient β_{inel} (blue) as a function of the scattering length a for a temperature $T = 500$ nK. Data points for β_{el} are marked (open symbols) when the number of K atoms increases during the measurement, and therefore our model, which ignores K-dimer elastic collisions, does not apply. The red dashed line shows the expected a^6 scaling in the halo regime according to the simplified theory. The blue dashed line shows the $a^{2.58}$ scaling which is deduced from a fit to the loss coefficients in the first set of measurement. The vertical error bars for the inelastic and elastic collision rates are given by the error of the fit. The horizontal error bars result from a 15-mG uncertainty in the magnetic field. A systematic error of 30% in the collision-rate coefficients is expected from a 10% error in the trapping frequency. The rate coefficient for elastic collisions for $a = -37\,a_0$, $322\,a_0$ lie outside of the plotting range. (b), (c) Effective temperatures T_z (dark gray) and T_x (light gray) as a function of the hold time for magnetic fields of 72.25 G ($-37\,a_0$), 77.25 G ($610\,a_0$).

Due to cross-dimensional thermalization, the temperatures in the two directions approach each other during the measurement [see Fig. 3(c)].

Unfortunately, our measurement does not allow us to quantitatively extract the scaling of β_{el} with the scattering length a in the halo regime due to the following two reasons. First, even though we intentionally reduced the initial molecule density to $n_0 = 0.4 \times 10^{11}$ cm^{-3}, the elastic collision rate becomes comparable to the trap frequencies for a scattering length of $a > 2000\,a_0$. Therefore the system enters the hydrodynamic regime and the measured value of β_{el} saturates near the so-called hydrodynamic limit given by $\bar{\omega}\alpha/(2\pi n_0) = 1.71 \times 10^{-9}$ cm^3/s with a geometric mean trapping frequency $\bar{\omega} = 2\pi \times 167$ Hz [32]. We note that in the presence of strong loss, the measured elastic collision rate can exceed the hydrodynamic limit calculated for a constant density. Second, our model, which only considers dimer-dimer elastic collisions, is only valid in deducing β_{el} for scattering lengths up to $610\,a_0$. When $a > 610\,a_0$, we observe an accumulation of spectator K atoms which can contribute to the cross thermalization. Due to these limitations, we see a strong deviation from the expected a^6 scaling. Nevertheless, this measurement shows that the rate
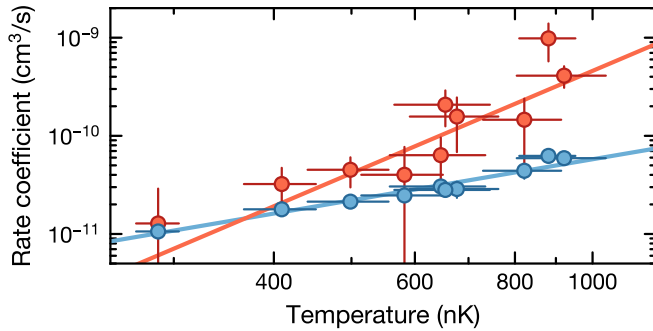
FIG. 4. Elastic p-wave collisions in fermionic Feshbach molecules for different temperatures. Elastic collision coefficient β_{el} (red) and inelastic collision coefficient β_{inel} (blue) as a function of the temperature averaged during the hold time for a scattering length $a = 610\,a_0$. The vertical error bars are given by the error of the fit. The horizontal error bars represent the statistical error of T_{avg} during the hold time. A systematic error of 30% in the collision rate is expected from a 10% error in the trapping frequency. The blue and red solid line are the fits of the polynomial function to the rate coefficients.

coefficient of elastic collisions exhibits a stronger scaling with the scattering length than that of inelastic collisions.

In addition, we measure the scaling of the elastic collision rate with the temperature. To this end we perform the nonadiabatic compression to different trap depths while keeping the ratio between the trapping frequencies fixed. To ensure that cross-dimensional thermalization results from elastic collisions between the Feshbach molecules, we perform the measurement at a scattering length of $a = 610\,a_0$, where we checked that the number of K atoms does not systematically change for the different temperatures. The results are summarized in Fig. 4. One can see that the elastic rate coefficient scales stronger with temperature compared to the inelastic one. For temperatures around $T = 300\,\mathrm{nK}$, the rates of elastic and inelastic collisions are comparable, while for $T = 1000\,\mathrm{nK}$, the elastic collision rate is larger by almost one order of magnitude. We fit the temperature scaling with the polynomial cT^{l_T} and obtain $l_T = 1.39(12)$ and $l = 3.46(63)\ l_T = 3.46(63)$ for β_{inel} and β_{el}, respectively. The measured temperature scaling of the elastic collision rate is faster than the $T^{5/2}$ scaling expected for p-wave collisions, pointing to nonuniversal collisional behavior.

IV. CONCLUSION

In conclusion, we have characterized inelastic and elastic collisions of fermionic NaK Feshbach molecules and found reasonable agreement with the threshold behavior of p-wave collisions between Feshbach molecules. The measured scalings qualitatively agree in the halo regime with the calculation for molecules that consist of two atoms with high mass imbalance. Our investigations in both the halo and the nonhalo regime provide a benchmark for calculations of the four-body problem that predict the collisional behavior in other heteronuclear molecules. The surprisingly strong suppression of dimer-dimer loss in the nonhalo regime suggests that after molecule formation, dimer loss can be strongly reduced by

quenching the magnetic field into the regime of large binding energies. This has, for example, been essential in our recent work on the generation of degenerate Fermi gases of NaK molecules [33,34].

With the discovery of long-lived interacting Feshbach molecules, it seems unfortunate that the pursuit for utilizing these molecules for quantum many-body physics has predominantly ceased. Further improvement of the ratio of elastic-to-inelastic collisions is expected when confining the molecules in two-dimensional traps [9,35], which should allow for evaporative cooling of Feshbach molecules and possibly the observation of p-wave paired phases. The authors of Ref. [9] have identified $^{40}\mathrm{K} - ^{39}\mathrm{K}$ as a promising system in this regard. Furthermore, it would be interesting to prepare fermionic Feshbach molecules formed by two magnetic atoms such as $^{170}\mathrm{Er}\,^{161}\mathrm{Dy}$ [36], which are expected to be long lived and exhibit large magnetic dipole moments [37].

APPENDIX A: LOCAL SCALING OF THE INELASTIC DIMER-DIMER COLLISIONS

As can be seen from Fig. 1 in the main text, the inelastic rate coefficient β_{inel} shows three regimes. In the nonhalo regime, β_{inel} is constant, while in the halo regime, it is expected to scale as $\beta_{\mathrm{inel}} \propto a^3$. In between, there is a transition regime. The exponent l_a therefore depends on the region in which the fit is performed. When using the data for $a > 1000\,a_0$, we find $l_a = 2.58(14)$, smaller than the expected value. However, by choosing different fit regions, we can show that the exponent indeed converges to $l_a \approx 3$ at higher scattering lengths. To do this we perform multiple fits, each time using only five consecutive data points from Fig. 1. The resulting exponents are plotted versus the fit region in Fig. 5. As expected, the exponent is close to 0 for small a, then increases to nearly 3 at the top end of the probed range. Interestingly, while one expects a monotonous increase of l_a from the nonhalo to the halo regime, the increase of l_a seems to pause in the regime between $200\,a_0$ and $700\,a_0$. This behavior might be the result of a potential Efimov resonance that causes deviations from the universal scaling p-wave collisions. We note that anomalous temperature dependencies of dimer-dimer collisions were previously observed with bosonic Cs_2 [5] and NaRb [29] Feshbach molecules at around $500\,a_0$.

APPENDIX B: EFFECT OF UNBOUND ATOMS ON THE DIMER-DIMER LOSS MEASUREMENT

In our measurements we detect the Feshbach molecules in time of flight using a Stern–Gerlach separation technique.
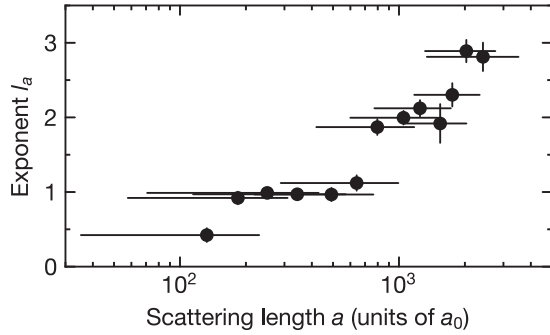
FIG. 5. Local scaling of the dimer-dimer loss on the scattering length. We extract the local exponent l_a as a function of the scattering length from Fig. 1 in the main text by considering the data of the inelastic collision-rate coefficient β_{inel} in the regime indicated by the horizontal bars. The error bars in the vertical direction show the error of the fit.

This allows us to determine the number of Feshbach molecules and atoms individually [33]. While we clearly do not observe unbound atoms for short hold times, we potentially see an accumulation of atoms for longer hold times. The number of accumulated atoms strongly depends on the interspecies scattering length a and thus on the binding energy of the Feshbach molecules.

The accumulation of K atoms can be understood from the underlying Na-Na-K three-body loss when two NaK Feshbach molecules collide. In this process, two Na atoms and one K atom form a short-lived trimer. In the consequent breakup, the binding energy of the trimer, on the order of 100 mK, is carried away by the atomic constituents [16], leading to their immediate escape from the trap. The remaining K atom in the collision acts as a spectator and takes away kinetic energy of about the binding energy of the Feshbach molecule $E_b = \hbar^2/(2\mu a^2)$. Thus the accumulation of K atoms is expected once the binding energy is less than the trap depth $U = k_B \times 6\,\mu\mathrm{K}$. The accumulation of Na atoms is caused by thermal dissociation of dimers. Once the binding energy of the dimers becomes comparable to the temperature, the collisional energy is large enough to break one of the dimers into their atomic constituents which subsequently remain in the trap.

Figure 6 shows the number of accumulated atoms during *longest holding times* as a function of the scattering length a for the measurements presented in Fig. 1 of the main text. We can identify three regions in this plot. For scattering length below $a < 350\,a_0$, we see no accumulation of atoms. Here the binding energy of the Feshbach molecules is larger than the trap depth. For scattering lengths $a > 350\,a_0$ where the binding energy is smaller than the trap depth, K atoms start to accumulate in the trap. The number of K atoms remains below 1000 until the binding energy becomes lower than the average kinetic energy $k_B T = k_B \times 500\,\mathrm{nK}$ at $a > 1300\,a_0$. In this regime the number of K atoms strongly increases, and Na atoms also start to accumulate in the trap. Here the thermal energy can suffice for the molecules to break apart into atomic constituents, whereas it is not large enough for the atoms to leave the trap. If this thermal dissociation is the dominant
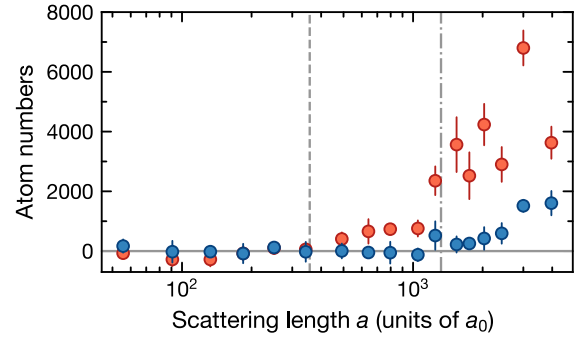

FIG. 6. Unbound atoms from three-body recombination and thermal dissociation. Number of accumulated Na atoms (blue) and K atoms (red) for the loss measurements presented in Fig. 1 at various scattering lengths a. For each measurement we prepare the system under the same conditions and average over the number of unbound Na or K atoms for the respective longest four holding times. The error bar indicates the standard deviation. The dashed line shows $E_b = U$, where $U = k_B \times 6\,\mu\mathrm{K}$ is the effective trap depth. The dash-dotted line indicates $E_b = k_B T$, where $T = 500\,\mathrm{nK}$ is approximately the temperature of the molecular sample.

process for the accumulation of unbound atoms, we might expect the detected number of K and Na atoms to be roughly the same. While our data does not seem to confirm this behavior, we note that this is likely a result of the Na-dimer loss being much larger than the K-dimer loss. This is illustrated in Fig. 7.

Based on the number of accumulated atoms and the atom-dimer loss coefficients presented in Fig. 7, we can estimate the effect of atom-dimer collisions on the measurements of the inelastic dimer-dimer collision-rate coefficient. As discussed in the main text, we ignore the effect of the accumulated K atoms on the inelastic dimer-dimer collisions. We justify this by the negligible number of K atoms for most scattering lengths. Close to resonance the number of K atoms becomes at most comparable to the number of Feshbach molecules. However, as shown in Fig. 7, in this regime the rate coefficient of inelastic K-NaK collisions is about two orders of magnitude smaller than the extracted coefficient of inelastic dimer-dimer collisions. While the number of Na atoms also remains negligible for most scattering lengths, close to
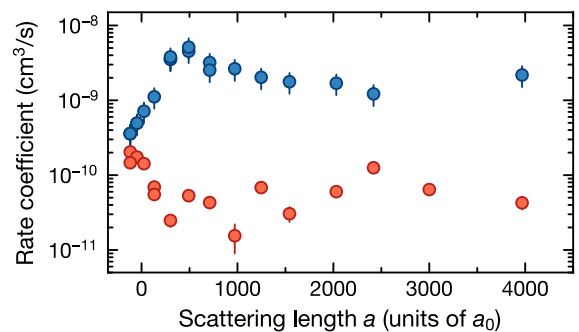

FIG. 7. Rate coefficients for Na-NaK (blue) and K-NaK (red) atom-dimer loss as a function of the scattering length measured at a temperature of 250 nK. The Na-NaK data is adapted from the Supplemental Material of Ref. [18].

resonance we do detect a noticeable number of accumulated Na atoms. In addition, the Na-NaK loss rate coefficient is comparable to the dimer-dimer loss rate coefficient. We estimate the *upper bound* of the Na-NaK contribution to the measured β_{inel} at 4000 a_0, where we expect the highest atom-dimer losses. We consider that the number of K atoms at the end of the loss measurement gives us an upper boundary of thermally dissociated Na atoms, which amounts to about 5000 atoms, as the thermally dissociated K atoms do not undergo collisional loss with the molecules near the resonance. We also consider that these 5000 Na atoms can undergo loss with the Feshbach molecules. If the rate coefficient of Na-dimer and dimer-dimer collisions is about the same, at most 15% of the measured β_{inel} comes from Na-dimer loss.

[1] L. D. Carr, D. DeMille, R. V. Krems, and J. Ye, Cold and ultracold molecules: Science, technology and applications, New J. Phys. **11**, 055049 (2009).

[2] G. Quéméner and P. S. Julienne, Ultracold molecules under control! Chem. Rev. **112**, 4949 (2012).

[3] J. L. Bohn, A. M. Rey, and J. Ye, Cold molecules: Progress in quantum engineering of chemistry and quantum matter, Science **357**, 1002 (2017).

[4] C. Chin, R. Grimm, P. Julienne, and E. Tiesinga, Feshbach resonances in ultracold gases, Rev. Mod. Phys. **82**, 1225 (2010).

[5] F. Ferlaino, S. Knoop, M. Mark, M. Berninger, H. Schöbel, H.-C. Nägerl, and R. Grimm, Collisions between Tunable Halo Dimers: Exploring an Elementary Four-Body Process with Identical Bosons, Phys. Rev. Lett. **101**, 023201 (2008).

[6] B. Marcelis, S. J. J. M. F. Kokkelmans, G. V. Shlyapnikov, and D. S. Petrov, Collisional properties of weakly bound heteronuclear dimers, Phys. Rev. A **77**, 032707 (2008).

[7] F. Ç. Top, Y. Margalit, and W. Ketterle, Spin-polarized fermions with *p*-wave interactions, Phys. Rev. A **104**, 043311 (2021).

[8] K. Maeda, G. Baym, and T. Hatsuda, Simulating Dense QCD Matter with Ultracold Atomic Boson-Fermion Mixtures, Phys. Rev. Lett. **103**, 085301 (2009).

[9] B. Bazak and D. S. Petrov, Stable *p*-Wave Resonant Two-Dimensional Fermi-Bose Dimers, Phys. Rev. Lett. **121**, 263001 (2018).

[10] M. Greiner, C. A. Regal, and D. S. Jin, Emergence of a molecular Bose–Einstein condensate from a Fermi gas, Nature (London) **426**, 537 (2003).

[11] C. A. Regal, M. Greiner, and D. S. Jin, Observation of Resonance Condensation of Fermionic Atom Pairs, Phys. Rev. Lett. **92**, 040403 (2004).

[12] J. J. Zirbel, K.-K. Ni, S. Ospelkaus, J. P. D'Incao, C. E. Wieman, J. Ye, and D. S. Jin, Collisional Stability of Fermionic Feshbach Molecules, Phys. Rev. Lett. **100**, 143201 (2008).

[13] C.-H. Wu, J. W. Park, P. Ahmadi, S. Will, and M. W. Zwierlein, Ultracold Fermionic Feshbach Molecules of ^{23}Na ^{40}K, Phys. Rev. Lett. **109**, 085301 (2012).

[14] M.-S. Heo, T. T. Wang, C. A. Christensen, T. M. Rvachov, D. A. Cotta, J.-H. Choi, Y.-R. Lee, and W. Ketterle, Formation of ultracold fermionic NaLi Feshbach molecules, Phys. Rev. A **86**, 021602(R) (2012).

[15] G. Barontini, C. Weber, F. Rabatti, J. Catani, G. Thalhammer, M. Inguscio, and F. Minardi, Observation of Heteronuclear Atomic Efimov Resonances, Phys. Rev. Lett. **103**, 043201 (2009).

[16] D. S. Petrov, Loss process in short range (private communication) (2021).

[17] G. Quéméner, Ultracold collisions of molecules, arXiv:1703.09174.

[18] X.-Y. Chen, M. Duda, A. Schindewolf, R. Bause, I. Bloch, and X.-Y. Luo, Suppression of Unitary Three-Body Loss in a Degenerate Bose-Fermi Mixture, Phys. Rev. Lett. **128**, 153401 (2022).

[19] See in Appendixes.

[20] A. Viel and A. Simoni, Feshbach resonances and weakly bound molecular states of boson-boson and boson-fermion NaK pairs, Phys. Rev. A **93**, 042701 (2016).

[21] R. Bause, A. Schindewolf, R. Tao, M. Duda, X.-Y. Chen, G. Quéméner, T. Karman, A. Christianen, I. Bloch, and X.-Y. Luo, Collisions of ultracold molecules in bright and dark optical dipole traps, Phys. Rev. Res. **3**, 033013 (2021).

[22] Z. Z. Yan, J. W. Park, Y. Ni, H. Loh, S. Will, T. Karman, and M. Zwierlein, Resonant Dipolar Collisions of Ultracold Molecules Induced by Microwave Dressing, Phys. Rev. Lett. **125**, 063401 (2020).

[23] S. Ospelkaus, K.-K. Ni, D. Wang, M. H. G. d. Miranda, B. Neyenhuis, G. Quéméner, P. S. Julienne, J. L. Bohn, D. S. Jin, and J. Ye, Quantum-state controlled chemical reactions of ultracold potassium-rubidium molecules, Science **327**, 853 (2010).

[24] E. R. Hudson, N. B. Gilfoy, S. Kotochigova, J. M. Sage, and D. DeMille, Inelastic Collisions of Ultracold Heteronuclear Molecules in an Optical Trap, Phys. Rev. Lett. **100**, 203201 (2008).

[25] Z. Idziaszek and P. S. Julienne, Universal Rate Constants for Reactive Collisions of Ultracold Molecules, Phys. Rev. Lett. **104**, 113202 (2010).

[26] A. Derevianko, J. F. Babb, and A. Dalgarno, High-precision calculations of van der Waals coefficients for heteronuclear alkali-metal dimers, Phys. Rev. A **63**, 052704 (2001).

[27] J. Mitroy and M. W. J. Bromley, Semiempirical calculation of van der Waals coefficients for alkali-metal and alkaline-earth-metal atoms, Phys. Rev. A **68**, 052714 (2003).

[28] P. S. Julienne, T. M. Hanna, and Z. Idziaszek, Universal ultracold collision rates for polar molecules of two alkali-metal atoms, Phys. Chem. Chem. Phys. **13**, 19114 (2011).

[29] F. Wang, X. Ye, M. Guo, D. Blume, and D. Wang, Observation of resonant scattering between ultracold heteronuclear Feshbach molecules, Phys. Rev. A **100**, 042706 (2019).

[30] K.-K. Ni, S. Ospelkaus, D. Wang, G. Quéméner, B. Neyenhuis, M. H. G. de Miranda, J. L. Bohn, J. Ye, and D. S. Jin, Dipolar collisions of polar molecules in the quantum regime, Nature (London) **464**, 1324 (2010).

[31] B. DeMarco, J. L. Bohn, J. P. Burke, M. Holland, and D. S. Jin, Measurement of *p*-Wave Threshold Law Using Evaporatively Cooled Fermionic Atoms, Phys. Rev. Lett. **82**, 4208 (1999).

[32] Z.-Y. Ma, A. M. Thomas, C. J. Foot, and S. L. Cornish, The evaporative cooling of a gas of caesium atoms in the hydrodynamic regime, J. Phys. B: At. Mol. Opt. Phys. **36**, 3533 (2003).

[33] M. Duda, X.-Y. Chen, A. Schindewolf, R. Bause, J. von Milczewski, R. Schmidt, I. Bloch, and X.-Y. Luo, Transition from a polaronic condensate to a degenerate Fermi gas of heteronuclear molecules, Nat. Phys. **19**, 720 (2023).

[34] A. Schindewolf, R. Bause, X.-Y. Chen, M. Duda, T. Karman, I. Bloch, and X.-Y. Luo, Evaporation of microwave-shielded polar molecules to quantum degeneracy, Nature (London) **607**, 677 (2022).

[35] Z. Zhang, L. Chen, K.-X. Yao, and C. Chin, Transition from an atomic to a molecular Bose–Einstein condensate, Nature (London) **592**, 708 (2021).

[36] G. Durastante, C. Politi, M. Sohmen, P. Ilzhöfer, M. J. Mark, M. A. Norcia, and F. Ferlaino, Feshbach resonances in an erbium-dysprosium dipolar mixture, Phys. Rev. A **102**, 033330 (2020).

[37] A. Frisch, M. Mark, K. Aikawa, S. Baier, R. Grimm, A. Petrov, S. Kotochigova, G. Quéméner, M. Lepers, O. Dulieu, and F. Ferlaino, Ultracold Dipolar Molecules Composed of Strongly Magnetic Atoms, Phys. Rev. Lett. **115**, 203201 (2015).